ID 197

ENVIRONMENTAL OPTIMIZATION OF ROTORCRAFT APPROACH TRAJECTORIES

Sander Hartjes, Hendrikus G. Visser, Marilena D. Pavel
s.hartjes@tudelft.nl, h.g.visser@tudelft.nl, m.d.pavel@tudelft.nl
Delft University of Technology, Delft, The Netherlands

Abstract
At the Delft University of Technology, an optimization framework is under development to optimize rotorcraft trajectories with respect to environmental and operational criteria. The new optimization framework comprises a dynamic trajectory optimization algorithm, a rotorcraft flight dynamics model, a geographic information system, a noise model and an emissions inventory model. The tool is largely based on past experience attained with the NOISHHH tool developed at the Delft University of Technology for the design of noise abatement procedures for fixed wing aircraft. The current paper presents the status of the developmental work through an illustrative example of a fictitious Simultaneous Non-Interfering approach trajectory at Amsterdam Airport Schiphol, which is optimized for several environmental and operational cost criteria.

Introduction
Increased public awareness of the negative impacts of aviation has led to an increased demand for improvements in the field of noise exposure and pollutant emissions. On an airport level, this has led to ever more stringent regulations, most specifically to reduce the noise impact on near-airport communities. Increasing landing fees and reducing or even disallowing operations of specific, noisy aircraft are amongst the measures taken. For the aircraft operators, these regulations and restrictions will increase operational cost, resulting in a complex balancing of environmentally friendly operations and operational costs.

In the specific case of rotorcraft, noise can be mainly attributed to mechanical components and aerodynamic phenomena such as Blade-Vortex Interaction. On a component level, *Yu et al.* [1] and *Lowson* [2], e.g., proposed passive rotor tip-shape modifications to reduce the aerodynamic noise, whereas amongst others *Fürst et al* [3], *Weems et al.* [4], and *Haber et al.* [5] propose several methods of active rotor controls to reduce the noise production. On the field of mechanical noise, *Yildirim et al.* [6] have shown promising results for noise reduction through improved transmission designs.

However, these findings can only be applied to future generation helicopters, or through upgrades on existing helicopters. With a possible application to the current generation of helicopters, significant improvements in noise and pollutant emissions can be achieved through the application of specific environmentally friendly helicopter procedures. In this field, the application of optimization techniques on point mass rotorcraft dynamics models by *Tsuchiya et al.* [7] has shown possible improvements on different noise impact criteria. In addition, *Bottasso et al. [8,9]* have shown the application of optimization techniques on more complex, rotorcraft models.

At Delft University of Technology, extensive research has been done in the field of aircraft trajectory optimization [10-12], and more recently in the field of helicopters [13] using the optimization tool NOISHHH. The current study tends to further expand the use of trajectory optimization techniques for rotorcraft based on NOISHHH. As a first step, the optimization algorithm used in NOISHHH has been replaced by a more advanced algorithm based on the software package GPOPS [14-21]. In addition, the point mass helicopter model in NOISHHH has been replaced by a rigid-body dynamic model with six degrees-of-freedom and quasi-static inflow of the main and tail rotors. This model also includes fuel and emissions modeling. Finally, the current version of the framework uses the same helicopter noise model as in NOISHHH, based on the Integrated Noise Model, version 7.0b.

To exemplify the current status of the development, the new tool, called RoTONoisE, has been applied to a fictitious Simultaneous Non-Interfering (SNI) approach trajectory to the helispot at Amsterdam Airport Schiphol (AAS).

Environmental Optimization
The current status of the RoTONoisE optimization framework allows for the optimization of rotorcraft trajectories with respect to time, fuel burn and gaseous pollutants. In addition, a number of noise impact criteria – both generic and site-specific – can be assessed through the implementation of a rotorcraft noise model.

When gaseous pollutants are considered, two categories need to be distinguished: 1) global emissions, which concern large-scale effects such as acid rain and global warming, and 2) local emissions, which concern the direct impact of emissions on, for instance, human health and the human environment. The latter are defined as pollutants emitted below the mixing height of 3,000 ft Above Ground Level (AGL). With the addition of a fuel flow model, however, it is also possible to assess and optimize the emission of carbon dioxide (CO_2) during the arrival trajectories. However, in this study, the main focus will be on operational cost criteria (fuel and time) and locally emitted nitrogen oxides (NO_x) emissions.

In order to optimize with respect to multiple criteria, and to be able to make a trade-off between environmental and operational cost considerations, a composite performance index has been defined which contains a weighted contribution of the various optimization criteria:

$$J = k_1 t_f + k_2 \int_{t_0}^{t_f} \sigma dt + k_3 \int_{t_0}^{t_f} EI_{NO_x} \sigma dt \qquad (1)$$

where σ is the fuel flow in kg·s^{-1}, EI_{NOx} the emission index for NO_x in g·kg^{-1}, and t_f in s, the final time of the problem. The weighting factors, $k_n \geq 0$, are used to make a trade-off between the different optimization criteria. Both the fuel flow and the emissions index for NO_x are derived from work done by the Swiss Federal Office of Civil Aviation (FOCA) [22]. In this study, only single objectives have been optimized, so $k_i = 1$, $k_{j\neq i} = 0$.

In an effort to reduce the computational burden of the problem, the total fuel burned and the total amount of NO_x emitted have been added as state variables. Although this increases the total problem size, it does not require the Lagrangian part of the performance index to be calculated separately, resulting in more efficient use of resources. As a result, however, the performance index should be rewritten as:

$$J = k_1 t_f + k_2 F_f + k_3 NO_{x,f} \qquad (2)$$

where F_f is the total fuel burned, and $NO_{x,f}$ is the total amount of NO_x emitted. Since expressing the fuel burn and the emissions of NO_x as a Mayer cost contribution results in the same numerical result as when using Lagrangian contribution, this adaptation does not affect the values of the weighting factors k_n.

Although not yet available for optimization, the RoTONoisE tool also allows the assessment of the noise impact on near-airport communities. For this purpose, population density data have been made available through a Geographic Information System (GIS) (see Figure 1) to allow the tool to assess the total number of people affected by the noise impact. The noise model currently implemented in RoTONoisE is derived from the Federal Aviation Administration (FAA) Integrated Noise Model, version 7b [23]. INM has been the FAA's standard methodology for noise assessment since 1979, and has been developed through a succession of versions. The current and final version of INM, version 7b, incorporates helicopter noise assessment based on the Heliport Noise Model (HNM).

To find the noise impact at a specific observer location, INM uses noise-power-distance (NPD) tables from which the selected noise metric can be found through interpolation over the slant range and the net corrected thrust. For the specific case of rotorcraft, the tables are not based on the engine power, but rather on the flight path angle of the helicopter. The tables are based on the assumption that the observer is standing directly below an aircraft passing in an infinitely long straight segment at a given reference speed. To correct for non-reference conditions, five adjustments are introduced: 1) the lateral directivity adjustment, to account for asymmetrical noise production, 2) the tip Mach number adjustment to correct for aerodynamic noise near the rotor-tip, 3) the noise fraction adjustment to account for finite-length segments, 4) the duration adjustment, which accounts for non-reference speeds for exposure based metrics such as the Sound Exposure Level, and 5) the lateral attenuation adjustment, which corrects for ground reflection and refraction, for observers not positioned directly below the flight path.

To determine the site-specific noise impact on near-airport communities, the concept of the *expected number of awakenings* is introduced. In order to determine this number, a dose-response relationship between the noise exposure and the expected percentage of awakenings due to a single nighttime flyover is combined with the population density data in the GIS. The dose-response relationship is based on research done by the Federal Interagency Committee on Aviation Noise (FICAN) in 1997 [24]. The resulting relationship, as shown in Figure 2, is based on laboratory tests and field experiments and provides an upper bound to the expected number of awakenings:

$$\%Awakenings = 0.0087\left(SEL - 30\right)^{1.79} \qquad (3)$$

where SEL is defined as the Sound Exposure Level in dBA that is experienced indoors. By combining the percentage awakenings with the actual population data in the GIS, the absolute number of people expected to awake due to a single night-time flyover can be determined.

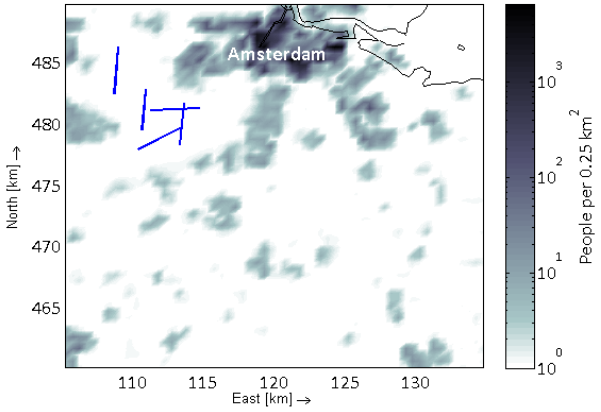

Figure 1: Population density around AAS

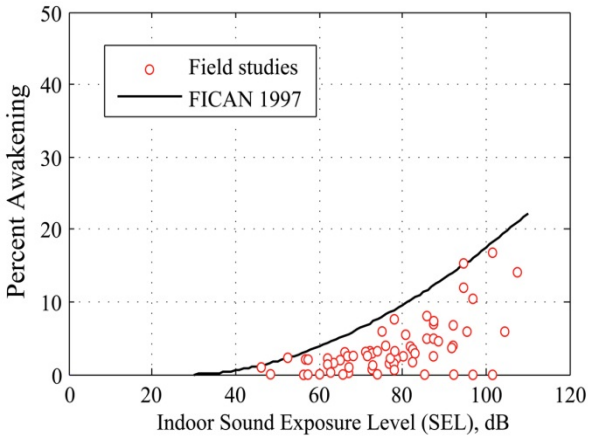

Figure 2: FICAN Proposed dose-response relationship

Figure 3: MBB Bo-105

Rotorcraft Flight Dynamics Model

The tool currently uses a rigid-body dynamic model with six degrees-of-freedom and quasi-static inflow of the main and tail rotors, based on the work by *Pavel* [25]. This model uses fourteen state variables {u, v, w, p, q, r, Φ, Θ, Ψ, x, y, z, $\lambda_{i,mr}$, $\lambda_{i,tr}$} representing the airspeed, rotational rates, body angles, position and quasi-dynamic inflow, respectively. The model is controlled by four control variables {θ_0, θ_{1s}, θ_{1c}, $\theta_{0,tr}$}, representing the blade collective pitch, longitudinal cyclic pitch, lateral cyclic pitch and tail rotor collective pitch, respectively. As mentioned before, both the fuel burned and the amount of NO_x emitted have been added as state variables to this model, in an effort to reduce the computational burden.

Although generic in nature, the current work is based on an MBB Bo-105 helicopter (see Figure 3). As a result, some performance constraints have been imposed, together with a variety of operational constraints and constraints for passenger comfort, which all apply to the complete trajectory. The total set of constraints is presented in Table 1.

Table 1: Trajectory constraints

Constraint	Inequality
Speed restriction	$V_{\min} \le \sqrt{u^2+v^2+w^2} \le V_{\max}$
Vertical speed	$\lvert w \rvert \le w_{\max}$
Acceleration	$\lvert \dot{V} \rvert \le 0.1g$
Turn rate	$\lvert \dot{\chi} \rvert \le 3^{\circ}/\mathrm{sec}$
Vertical acceleration	$\lvert \dot{w} \rvert \le 0.15g$
Power constraint	$P_{req} \le P_{available}$

Numerical Methodology

The numerical trajectory optimization method implemented in RoTONoisE is a direct, pseudospectral optimization technique using orthogonal collocation with Non-Linear Programming (NLP). This method, called the Radau Pseudospectral Method (RPM), which is enveloped in the software tool GPOPS [14-21], essentially transforms the continuous optimal control problem into an NLP formulation by discretizing the trajectory dynamics. For this purpose, the vehicle's state and control variables are first discretized using Lagrangian interpolation. To accurately approximate the dynamics of the problem, the RPM uses Radau Quadrature. As a result, the discretization points used in the RPM, called nodes, are defined on the interval $\tau \in [-1,\ldots,1]$, as the roots of the Legendre polynomials $P_k(\tau)$-$P_{k-1}(\tau)$, with

$$\tau = \frac{2t}{t_f - t_0} - \frac{t_f + t_0}{t_f - t_0} \qquad (4)$$

After discretization, the next step is to collocate the state derivatives with the dynamic constraints imposed on the problem. The values of the states and controls at the collocation points are then treated as a set of NLP variables.

Finally, path and control constraints imposed on the problem are treated as inequalities in the NLP formulation.

The resulting NLP problem definition is then solved with the numerical solver SNOPT [26]. In contrast to the collocation method used in NOISHHH, the resulting optimal trajectories are characterized by continuous control and state histories, expressed as Lagrange polynomials.

The number of nodes chosen to define the trajectory is of great influence on the accuracy of the results, and on the computational burden of the problem. Compared to previous work done with NOISHHH, optimization in RoTONoisE requires a relatively large number of nodes to better model the vehicle's dynamics. As a result, the examples presented herein have been discretized at 60 nodes, resulting in an NLP problem with 1238 non-linear variables and 1343 non-linear constraints. The average runtime for a typical problem is then less than 10 minutes at a standard laptop CPU using a single-core at 2.10 GHz.

Control Damping

In the initial optimized trajectories it was found that the controller input showed bang-bang behavior, typically found in singular optimal control formulations, where the state equations are linear in the controls and the performance index does not contain control variables. From an operational perspective, this behavior is unrealistic and unacceptable. To counter this problem, a form of control damping has been applied to resolve this problem. The control is damped by adding the squared control rate to the performance index through:

$$J_u = k_4 \int_{t_0}^{t_f} \dot{u}^2 dt \qquad (5)$$

However, since the control rates are not directly available, the Lagrangian cost contribution expressed in Equation (5) needs to be approximated as a Mayer cost contribution. For this purpose, on each segment the control rate was approximated assuming a linear control

input over a segment. The integral is then approximated as

$$J_u = k_4 \int_{t_0}^{t_f} \dot{u}^2 dt \approx k_4 \sum_{i=1}^{n} \left(\frac{\Delta u_i}{\Delta t_i} \right)^2 \Delta t_i \qquad (6)$$

and added to the performance index seen in Equation (2). Here Δu_i and Δt_i are the change in control and time over the i^{th} segment. It is noted that the weighting factor k_4 is parametrically varied to ensure that the relative contribution of the control rates to the total performance index is within the same order of magnitude for all example cases. In addition, the weighting factor k_4 should be sufficiently large to have a significant effect, yet sufficiently small to not dominate the performance index, and influence the final results too much. It was found that choosing k_4 in such a way that the control damping had a 1% contribution to the total performance index showed desirable results.

Figure 4: Google Earth Overview of the example scenario

SNI Example Scenario at Amsterdam Airport Schiphol

To show the current state of the development of the RoTONoisE optimization framework, an example scenario is presented of a Simultaneous Non-Interfering approach to the helispot at AAS. This fictitious trajectory starts at the Schiphol CTR boundary at 8 NM from the airport, and originates from the southeast (see Figure 4).

The instrument approach procedures presently in use at AAS are optimized for fixed-wing aircraft. However, rotorcraft using the same procedures significantly affect the runway capacity due to their relatively low approach speeds. As an alternative concept, Simultaneous Non-Interfering approach procedures are adopted to allow approaching rotorcraft to avoid fixed-wing traffic routes.

To implement the various approach procedure segments, a so-called multi-phase problem definition has been used. This allows for different constraints and performance indices to be used in the individual phases. In this particular case, two phases are used. The initial arrival segment starts at 3,000 ft AGL at the Schiphol CTR boundary, and ends at 1,000 ft AGL. The initial airspeed is fixed at 110 kts.

The second phase consists of an Instrument Landing System (ILS) glideslope and localizer. In this particular case, the localizer runs almost parallel to Runway 27, at a fixed offset angle of 10°. The glideslope angle, however, is not predefined. Using so-called design parameters, the optimization algorithm is free to choose a glideslope angle between 3° and 10°. As a result, the initial and final positions of the second phase are also a function of the glideslope angle. The final altitude is at decision height, 200 ft AGL, on the glideslope. In addition to the constraints mentioned in Table 1, some additional constraints apply to this phase, shown in Table 2.

Table 2: Glideslope constraints

Constraint	Equality
Initial altitude	$h_0 = 3{,}000\ ft$
Final altitude	$h_f = 200\ ft$
Final airspeed	$V_f = 30\ kts$
Glideslope & Localizer	$x = x_f - R \sin \chi_{LOC} \cos \gamma_{GS}$
	$y = y_f - R \cos \chi_{LOC} \cos \gamma_{GS}$
	$z = z_f + R \sin \gamma_{GS}$

Here, χ_{LOC} is the localizer heading of 277°, and γ_{GS} the variable glideslope angle. The coordinates (x_f, y_f, z_f) define the location of the helispot, with R the slant range between the current position and the helispot.

Results

The example scenario presented in the previous section has been optimized with respect to all three available criteria. Furthermore, the noise impact on the local communities has been assessed as well. The major results of all test cases can be found in Table 3.

Table 3: Results of the optimized trajectories

	Time [s]	Fuel [kg]	NO_x [g]	Awakenings
Time	**218.55**	9.83	37.42	840.29
Fuel	221.17	**9.77**	36.24	850.73
NO_x	274.75	10.79	**32.42**	994.18

It follows from these results that the overall difference between the time and fuel cases is very small. Although a small time gain can be achieved with respect to the fuel optimized solution, the additional fuel cost for this gain is negligible. The high speeds in the fuel optimized trajectory can be explained by considering the power required of the helicopter. Although high speeds require a significantly higher power required – and as a result a high fuel flow in $kg \cdot s^{-1}$ – the simultaneous reduction of the total flight time leads to a lower fuel flow in $kg \cdot m^{-1}$, and hence a lower total fuel burn. The main differences between these solutions lie in the acceleration and deceleration. The helicopter is allowed to accelerate from the initial point, and has to decelerate during the glideslope phase. It is in these phases that the fuel optimized solution shows a smoother transition than the time optimized solution, to reduce the power required in these maneuvers. This can be seen from Figure 5.

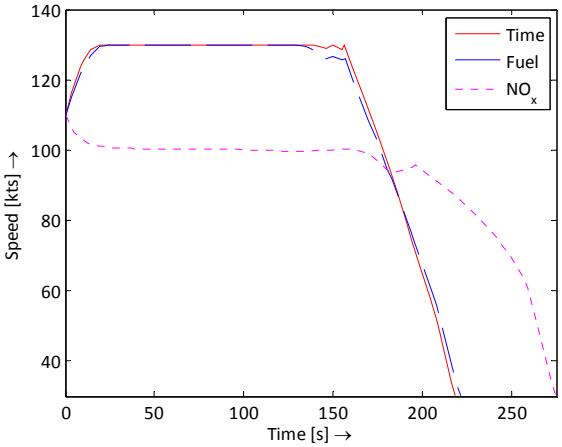

Figure 5: Airspeed profiles

Looking at the results of the NO_x optimized trajectory, a reduction of over 10% with respect to the fuel optimized solution has been found. In this case, increasing the power required and reducing the total flight time has a pronounced negative effect on the total NO_x emitted. As can be seen from Figure 5, there is clearly an optimum speed of around 100 knots at which the amount of NO_x emitted per meter is minimized. This logically also significantly affects the total flight time.

In addition, as mentioned before, the three trajectories presented herein feature a free glideslope angle. A steep glideslope results in a shorter trajectory, but also requires deceleration to the final airspeed of 30 kts over a shorter distance. As the time optimized solution only has to comply with deceleration constraints, it has the steepest glideslope at 5.25° to allow for the highest glideslope intercept speed. The fuel optimized solution follows at 5.18°. This minor difference is caused by the gentler deceleration in the fuel optimized trajectory to reduce the power required in this maneuver. Finally, the NO_x optimized solution has a glideslope of 4.66°. Having the strongest coupling between power required and the performance index, it requires a significantly slower airspeed and lower deceleration to minimize the NO_x emitted. Logically, since all three objectives benefit from a short trajectory, the resulting trajectories are very similar, as can be seen from the Google Earth overview of the three trajectories, presented in Figure 6.

Figure 6: Time, fuel and NO_x optimized trajectories

Finally, the noise impact of the three trajectories was also assessed. Since the routing of the three trajectories is very similar, the main gain in the number of expected awakenings results from the airspeed. Since the number of awakenings is based on the Sound Exposure Level, and hence is dependent on the exposure time, a fast trajectory will result in a lower exposure time and a lower number of awakenings. This can clearly be seen from Table 3. Although it is not yet possible to optimize with respect to any noise criterion in RoTONoisE, previous research into a similar SNI departure [13] has shown that approaching over the A9 highway and avoiding the populated areas significantly reduces the number of awakenings (see Figure 7). To analyze this effect, but more importantly to assess the capability of RoTONoisE to handle a complex set of constraints, a fuel optimized trajectory was forced to fly partly over the highway. As can be seen in Figure 7, the constrained trajectory clearly follows a large part of the highway.

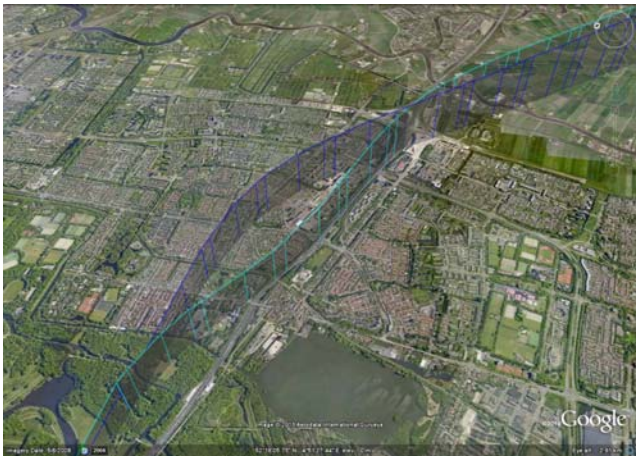

Figure 7: Detail of the constrained fuel optimized trajectory

Table 4: Results of two fuel optimized trajectories

	Time [s]	Fuel [kg]	NO_x [g]	Awakenings
Fuel	221.17	**9.77**	36.24	850.73
Highway	229.31	10.04	36.85	**933.83**

However, looking at the results presented in Table 4, it can directly be seen that the new trajectory is performing significantly worse with respect to the number of awakenings, and in fact with respect to all four criteria. Although this last test-case was merely a test of the functional capabilities of RoTONoisE, it is still relevant to assess these results. The reason for the increased number of awakenings in this case is twofold: firstly, the solutions found in previous research were *optimized* with respect to awakenings, which implies that not only the ground track, but also the speed and altitude profiles were optimized for noise. The ground track of the trajectory presented herein is diverted, but the speed and altitude profiles are still optimized with respect to fuel. Secondly, the relatively sharp turn required to leave the highway and intercept the localizer requires the airspeed to be relatively low. This, in combination with a steep glideslope angle of 7.39° results in a glideslope intercept speed of

around 90 knots, whereas the airspeed of the unconstrained solution is still 126 knots at that point. This significantly reduced airspeed increases the noise exposure time, and as a result increases the number of expected awakenings.

Conclusions

The work presented herein aimed to show the capabilities of the RoTONoisE rotorcraft trajectory optimization tool, currently under development at the Delft University of Technology.

It has been shown that with the current status of the tool, rotorcraft trajectories can be successfully optimized with respect to fuel burn, time and NO_x emissions, whilst maintaining relatively short runtimes and higher fidelity rotorcraft modeling as compared to previous research.

In addition, it has been shown that the tool is fully capable of imposing a complex set of constraint on the problem. Although the constraints used in this particular work may not be realistic from an operational perspective, there is no indication that imposing different constraints will have a negative effect on the ability of the tool to find an optimized trajectory.

Future Work

As stated before, the RoTONoisE optimization framework is a work in progress, and requires a number of improvements in the fields of rotorcraft modeling, noise modeling and the assessment of operationally more realistic trajectories.

As a first step for further development of the tool, the INM noise model will be implemented within the optimization routine, to allow for basic optimization with respect to noise. In addition, in parallel to this project, a more accurate noise model is being developed. This model, developed in cooperation with Roma III University in Rome, will be a trade-off between computational burden and numerical accuracy, and will be based on a high-fidelity noise source model in conjunction with a noise propagation model that essentially implements an analytical approximation of ray-tracing methods. This model will significantly increase the accuracy of the noise optimization within RoTONoisE, whilst minimally affecting the computation times.

Secondly, to be able to assess the optimized trajectories for different types of helicopters, the tool will be extended to include different types of helicopters, starting with the SA 330 Puma.

Finally, as it is expected that noise optimization and the assessment of more complex test-cases will significantly increase the computation time, large parts of the RoTONoisE code will be translated to a more efficient programming language.

It is anticipated that the fully mature tool can be used to optimize similar rotorcraft trajectories as presented in this paper, but with significantly more realistic trajectories with respect to operational constraints and pilot acceptance.

References

[1]Yu, Y.H., Liu, S.R., Jordan, D.E., Landgrebe, A.J., Lorber, P.F., Pollack, M.J., and Martin, R.M., "*Aerodynamic Acoustic Test of a United Technologies Model Scale Rotor at DNW"*, Proceedings, 46th American Helicopter Society Annual Forum, 1990

[2]Lowson, M.V., *"Progress Towards Quieter Civil Helicopters"*, Proceedings, 17th European Rotorcraft Forum, 1991

[3]Fürst, D., Keßler, C., Auspitzer, T., Müller, M., Hausberg, A., and Witte, H., *"Closed Loop IBC-System and Flight Test, Results On The CH-53G Helicopter"*, Proceedings, 60th American Helicopter Society Annual Forum, 2004

[4]Weems, D.B., Anderson, D.M., Mathew, M.B., and Bussom, R.C., *"A Large-Scale Active-Twist Rotor"*, Proceedings, 60th American Helicopter Society Annual Forum, 2004

[5]Haber, A., Jacklin, S., and Simone, G., *"Development, Manufacturing, and Component Testing of an Individual Blade Control System for a UH-60 Helicopter Rotor",* Proceedings, American Helicopter Society Aerodynamics, Acoustics, and Test and Evaluation Specialists Meeting, 2002

[6]Yildirim, N., Gasparini, G., Sartori, S., *"An Improvement on Helicopter Transmission Performance Through Use of High Contact Ratio Spur Gears with Suitable Profile Modification Design",* Proceedings of the Institution of Mechanical Engineers, Part G: Journal of Aerospace Engineering, **222**(8), pp. 1193-1210, 2008

[7]Tsuchiya, T., Ishii, H., Uchida, J., Ikaida, H., Gomi, H., Matayoshi, N., and Okuno, Y., *"Flight Trajectory Optimization to Minimize Ground Noise in Helicopter Landing Approach"*, Journal of Guidance, Control, and Dynamics, **32**(2), pp. 605-615, 2009

[8]Bottasso, C.L., Croce, A., Leonello, D., Riviello, L., *"Optimizatin of Critical Trajectories for Rotorcraft Vehicles*", Jorunal of the American Helicopter Society, **50**, pp. 165-177, 2005

[9]Bottasso, C.L., Croce, A., Leonello, D., Riviello, L., *"Rotorcraft Trajectory Optimization with Realizability Considerations"*, Journal of Aerospace Engineering, **18**, pp. 145-155, 2005

[10]Visser, H.G., Wijnen, R.A.A., *"Optimization of Noise Abatement Arrival Trajectories"*, Proceedings, AIAA Guidance, Control, and Control Conference and Exhibit, Montral, 2001

[11]Visser, H.G., Wijnen, R.A.A., *"Optimization of Noise Abatement Departure Trajectories"*, Journal of Aircraft, **38**(4), 2001

[12]Hartjes, S., Visser, H.G., and Hebly, S.J., *"Optimisation of RNAV Noise and Emission Abatement Standard Instrument Departures"*, The Aeronautical Journal, **114**(1162), 2011

[13]Visser, H.G., Pavel, M.D., and Tang, S.F., *"Optimization of Rotorcraft Simultaneous Non-Interfering Noise Abatement Approach Procedures"*, Journal of Aircraft, **46**(6), 2009

[14]Rao, A.V., Benson, D.A., Darby, C.L., Patterson, M.A., Francolin, C., sanders, I., Huntington, G.T., *"Algorithm*

902: GPOPS, A MATLAB Software for Solving Multiple-Phase Optimal Control Problems Using the Gauss Pseudospectral Method", ACM Transactions on Mathematical Software, **37**(2), pp. 22.1-22.39, 2010

[15]Garg, D., Patterson, M.A., Hager, W.W., Rao, A.V., Benson, D.A., Huntington, G.T., *"A Unified Framework for the Numerical Solution of Optimal Control Problems Using Pseudospectral Methods"*, Automatica, **46**(11), pp. 1843-1851, 2009

[16]Benson, D.A., *"A Gauss Pseudospectral Transcription for Optimal Control"*, Ph.D. Thesis, Departement of Aeronautics and Astronautics, Massachusetts Institute of Technology, 2004

[17]Huntington, G.T., "Advancement and Analysis of a Gauss Pseudospectral Transcription for Optimal Control", *Ph.D. Thesis*, Departement of Aeronautics and Astronautics, Massachusetts Institute of Technology, 2007

[18]Benson, D.A., Huntington, G.T., Thorvaldsen, T.P., Rao, A.V., *"Direct Trajectory Optimization and Costate Estimation via an Orthogonal Collocation Method"*, Journal of Guidance, Control, and Dynamics, **29**(6), pp. 1435-1440, 2006

[19]Huntington, G.T., Benson, D.A., Rao, A.V., *"Design of Optimal Tetrahedral Spacecraft Formations"*, The Journal of the Astronautical Sciences, **55**(2), pp. 141-169, 2007

[20]Huntington, G.T., Rao, A.V., *"Optimal Reconfiguration of Spacecraft Formations Using a Gauss Pseudospectral Method"*, Journal of Guidance, Control, and Dynamics, **31**(3), pp. 689-698, 2008

[21]Huntington, G.T., Benson, D.A., How, J.P., Kanizay, N., Darby, C.L., Rao, A.V., *"Computation of Boundary Controls Using a Gauss Pseudospectral Method",* Proceedings, Astrodynamics Specialist Conference, 2007

[22]FOCA, *"Guidance on the Determination of Helicopter Emissions"*, Edition 1, 2009

[23]Office of Environment and Energy, Integrated Noise Model Version 7.0 Technical Manual, FAA-AEE-08-01, USA, 2008

[24]Federal Interagency Committee on Aviation Noise (FICAN), *"Sleep Disturbance Caused by Aviation Noise"*, USA, 1997

[25]Pavel, M.D., *"On the Necessary Degrees of Freedom for Helicopter and Wind Turbine Low-Frequency Mode Modeling"*, PhD Thesis, Delft University of Technology, 2001

[26]Gill, P.E., Murray, W., and Saunders, M.A. (2008), *"User's Guide for SNOPT Version 7: Software for Large-Scale Nonlinear Programming",* Departement of Mathematics, University of California, San Diego, La Jolla